TA4 – Radiation Protection at Workplaces

APPLICATION OF COMBINED TLD AND CR-39 PNTD METHOD FOR MEASUREMENT OF TOTAL DOSE AND DOSE EQUIVALENT ON ISS

E. R. Benton[1], S. Deme[2], and I. Apathy[2]
[1]Eril Research, Inc., Stillwater, Oklahoma, USA
[2]KFKI Atomic Energy Research Institute, Budapest, Hungary

Abstract: To date, no single passive detector has been found that measures dose equivalent from ionizing radiation exposure in low-Earth orbit. We have developed the ISS Passive Dosimetry System (PDS), utilizing a combination of TLD in the form of the self-contained Pille TLD system and stacks of CR-39 plastic nuclear track detector (PNTD) oriented in three mutually orthogonal directions, to measure total dose and dose equivalent aboard the International Space Station (ISS).

The Pille TLD system, consisting on an on board reader and a large number of Ca_2SO_4:Dy TLD cells, is used to measure absorbed dose. The Pille TLD cells are read out and annealed by the ISS crew on orbit, such that dose information for any time period or condition, e.g. for EVA or following a solar particle event, is immediately available.

Near-tissue equivalent CR-39 PNTD provides LET spectrum, dose, and dose equivalent from charged particles of $LET_\infty H_2O \geq 10$ keV/μm, including the secondaries produced in interactions with high-energy neutrons. Dose information from CR-39 PNTD is used to correct the absorbed dose component ≥10 keV/μm measured in TLD to obtain total dose. Dose equivalent from CR-39 PNTD is combined with the dose component <10 keV/μm measured in TLD to obtain total dose equivalent.

Dose rates ranging from 165 to 250 μGy/day and dose equivalent rates ranging from 340 to 450 μSv/day were measured aboard ISS during the Expedition 2 mission in 2001. Results from the PDS are consistent with those from other passive detectors tested as part of the ground-based ICCHIBAN intercomparison of space radiation dosimeters.

Introduction

Passive radiation detectors possess a number of distinct advantages over active radiation detectors when it comes to personnel dosimetry. The principal advantages of passive detectors are their small size and mass, and their ability to function without a source of external power. Personnel dosimeters can take the form of light weight "badges" that can be worn on the body without hindering an individual's ability to do move about freely. The advantages of passive detectors over active detectors for personnel dosimetry are even more pronounced in the context of the space radiation *environment and, today, all of the world's space agencies with human space flight programs use some form of passive dosimeter to monitor crew radiation exposure in space. Passive detectors have also been widely used for area dosimetry throughout the habitable volume of spacecraft. Their lack of a power requirement, in addition to their small size and low cost, means that relatively large numbers of passive radiation detectors can be distributed throughout a spacecraft in order to monitor the radiation environment as a function of location, shielding, and other variables.*

There are, nonetheless, a number of limitations to the use of passive detectors as personal crew dosimeters for cosmonauts and astronauts. One limitation is the fact that passive radiation detectors must be returned to the ground for processing and analysis. Another limitation stems from the complexity of the radiation field encountered aboard spacecraft. The space radiation environment consists of both primary charged particles and secondary charged and neutral particles that span a wide range of energies. No single type of passive detector has been found that is sensitive to all the relevant types of radiation over the energy range of significance for dosimetry. A radiation dosimeter for crew and area monitoring must be sensitive to electrons of energy up to ~6 MeV, protons of energy ranging from a few MeV to over a GeV (HZE particles), to heavy ions of charge ≥2 at energies from 10's of MeV/amu to several GeV/amu, as well as a wide range of secondary particles formed when the primary radiation interacts with the mass of the spacecraft and its contents. These secondary particles include γ-rays and x-rays, and charged particle secondaries over a wide range of energies. A passive radiation dosimeter should also possess a sensitivity to neutrons of energy less than 1 MeV to several hundred MeV similar to that of tissue. Details of the space radiation environment in low-Earth orbit (LEO) may be found in [Benton & Benton, 2001].

We have developed the Passive Dosimetry System (PDS) for radiation monitoring aboard the International Space Station (ISS). The PDS consists of a combination of near-tissue equivalent CR-39 plastic nuclear track detector (PNTD) and $CaSO_4$:Dy thermoluminescent detector (TLD). CR-39 PNTD is used to measure the LET spectrum, dose, and dose equivalent from particles of $LET_{\infty}H_2O$ ≥10 keV/μm. TLD in the form of the Pille on-board TLD system is used to measure absorbed dose, although it registers the dose from high-LET particles with reduced efficiency. Using the method described below, the fraction of the dose from high-LET particles is subtracted from the TLD measurement. The dose in TLD from low-LET radiation is then added to the dose from particles of $LET_{\infty}H_2O$ ≥10 keV/μm measured in CR-39 PNTD to obtain total dose, and is added to the dose equivalent from particles of $LET_{\infty}H_2O$ ≥10 keV/μm measured in CR-39 PNTD to obtain total dose equivalent. Using this combination of two passive radiation detectors, we are able to monitor that portion of the space radiation environment relevant to crew dosimetry. While the CR-39 PNTD detector stacks contained in each PDS dosimeter still needs to be returned to the ground for processing and analysis, the use of the self-contained

Pille TLD system permits the TLD portion of the PDS to be read out, annealed, and reused while on-orbit. The use of the Pille TLD system also allows for the measurement of dose received by astronauts and cosmonauts during EVA, as described in the companion paper [Deme et al., 2006]. Further details regarding the use of CR-39 PNTD in combination with TLD for space radiation dosimetry may be found in [Benton et al., 2002]. Details regarding the Pille on-board TLD system may be found in [Feher et al., 1981] and [Apathy et al., 1996].

The PDS was first used aboard the ISS during the Expedition 2 DOSMAP experiment in 2001. Twelve PDS dosimeters were exposed throughout the U.S. Lab and Node 1 modules of ISS during a 100 day experiment. Passive and active radiation detectors from other laboratories were also exposed inside the ISS during this time as part of DOSMAP and other experiments.

Experiment

The ISS Passive Dosimetry System consists of an on-board Pille TLD reader and a number of PDS dosimeters. Each PDS dosimeter consists of a Pille TLD cell surrounded by three mutually-orthogonal stacks of CR-39 PNTD. The TLD cell containing $CaSO_4$:Dy is mounted in an aluminum/nomex holder. The three CR-39 PNTD stacks are placed in pockets on two of the sides and at the end of the holder. The PDS dosimeter is attached by Velcro to a location inside the ISS. The dosimeter remains in this semi-permanent position for the duration of the experiment. The Pille TLD bulb can be removed from the holder for readout by the Pille reader at suitable intervals over the course of the experiment. The three stacks of CR-39 PNTD can be exchanged during regular crew rotation when a Space Shuttle or Soyuz vehicle is docked to the station. Following the return of the CR-39 stacks to the ground, processing, readout and analysis are carried out in the laboratory. Figure 1 shows an example of a PDS dosimeter.

Figure 1. PDS Dosimeter: The Pille TLD A0012 is mounted in an aluminum/nomex holder which contains the stacks of CR-39 PNTDs in pockets at the bottom, far-side, and right end of the holder.

For the 2001 DOSMAP experiment, the Pille TLD and CR-39 PNTD components of the PDS were delivered to ISS at different times. The Pille TLD reader and a full complement of TLD dosimeter cells were delivered to ISS on STS-102/5A.1 on 8 March 2001, after which they were placed in storage. The PDS Supply/Return Kit, including the CR-39 PNTD stacks in their PDS holders, were delivered inside the MPLM to ISS on 19 April 2001, transferred to the US Lab on 26 April 2001, and then moved to the HRF rack in the US Lab on 29 April 2001. On 3 May 2001, the Pille TLDs were annealed and inserted into the PDS holders. The PDS holders were then distributed throughout the US Lab and Node 1. During the course of the DOSMAP experiment, the Pille TLDs were read out on ten separate occasions. One of the Pille TLD cells (A0101) was left inside the Pille reader and was automatically read out once every 90 minutes over the course of the DOSMAP experiment. On 9 August 2001, the PDS dosimeters were collected and the Pille TLDs read out for a final time. The PDS holders, including the CR-39 PNTD stacks, were returned to the Supply/Return Kit and stored on the Air Lock Deck of Node 1. On 22 August 2001, the PDS Supply/Return Kit was returned to the ground on STS-105/7A.1. The dose data measured by the Pille TLD reader was stored on a PCMCIA Flash Memory card, which was returned to the ground with the PDS Supply/Return Kit. The locations of the twelve PDS dosimeters throughout the U.S. Lab and Node 1 modules of ISS are listed in Table 1.

Following return of the CR-39 PNTD component of the PDS, two individual layers of CR-39 PNTD from each of the three orthogonal stacks in each PDS dosimeter were chemically etched in a solution of 50°C, 6.25 N NaOH for *periods of 36 hours and 7 days (168 hr), respectively. The 36 hour-processed (short-etch) detectors yielded track information from high-LET, short-range particles (>~8 μm), including neutron- and proton-induced target fragment recoils, as well as from primary HZE particles. The 7 day-processed (long-etch) detectors yielded information from longer-range particles (>~40 μm) in the lower LET portion of the spectrum above ≥5 keV/μm. The detectors are analyzed using a customized version of the ELBEK Automated Track Detector Analysis System [Noll et al., 1988; Rusch et al., 1991]. Track data was converted to LET spectrum utilizing an empirically derived function relating LET to the measured reduced etch rate ratio, V_R, for each track. The long-etch and short-etch detector data from the three orthogonal detector stacks were combined into average long-etch and short-etch LET spectra. Then the LRP and SRP spectra were then combined into a single LET spectrum in the interval from ~5 to 1500 keV/μm. The integral LET dose (Gy) and dose equivalent (Sv) spectra were determined by:*

$$D_{PNTD} = \frac{4\pi 1.602 \times 10^{-9}}{\rho} \sum_{i = 10\ keV/\mu m}^{max} f(i)LET(i),$$

and

$$H_{PNTD} = \frac{4\pi 1.602 \times 10^{-9}}{\rho} \sum_{i = 10\ keV/\mu m}^{max} f(i)\ Q(i)\ LET(i),$$

where ρ is the density of tissue and f(i) is the fluence of the particles with LET(i). The quality factor, Q(i), was determined using the ICRP-60 definition [ICRP, 1991].

Dose from particles of LET <10 keV/μm (Q = 1), measured by the Pille TLD cells was found by weighing the average dose from particles of $LET_\infty H_2O$ ≥10 keV/μm measured in CR-39 PNTD by an empirically-determined, LET-dependent dose registration efficiency function, η(i), for the $CaSO_4$:Dy TLD used in the Pille cells, and subtracting this quantity from the total absorbed dose measured by the Pille cell:

$$D_{Q=1} = D_{TLD} - \sum_{i = 10\ keV/\mu m}^{max} \eta(i) D_{PNTD}(i).$$

The total absorbed dose was found by:

$$D_{Total} = D_{Q=1} + D_{PNTD},$$

while the total dose equivalent was found by:

$$H_{Total} = D_{Q=1} + H_{PNTD}.$$

Average total dose rate and average total dose equivalent rate were determined by dividing total dose and total dose equivalent by the duration of the PDS exposure on ISS.

Results and Discussion

The locations of the twelve PDS dosimeters throughout the U.S. Lab and Node 1 modules of ISS are listed in Table 1. Table 1 also lists the average dose rates measured by the twelve Pille TLD cells in the PDS dosimeters. Average dose rates for ten of the twelve Pille TLD cells ranged from 160 to 190 μGy/d, while two Pille cells measured significantly higher average dose rates. The minimum dose rate was 160.8 μGy/d measured in PDS Dosimeter A0104 located near the forward hatch of the Node 1 module. The maximum dose rate of 242.6 μGy/d was measured in A0102 located near the aft hatch of Node 1. The other significantly high absorbed dose measurement was obtained for PDS Dosimeter A0101—239.5 μGy/d—which was permanently mounted in the Pille reader located in the HRF rack of the U.S. Lab and which was automatically read out once every 90 minutes. The differences in the average dose rates measured by the twelve Pille TLD cells largely reflect differences in the localized shielding environment surrounding each of the detectors. However, the East/West trapped proton anisotropy also likely contributed to some of the differences in the TLD dose results.

Figures 2, 3, and 4 show a representative samples of the LET spectra measured in the CR-39 PNTD exposed in the PDS dosimeters during the Expedition 2 DOSMAP experiment. Figure 2 shows the differential LET fluence spectra measured in the long-etch and short-etch CR-39 PNTD layers from PDS Dosimeter A0105, located near the HRF rack in the U.S. Lab. The differential LET spectrum from the long-etch detector is divided into two components—the spectrum from particles that produced tracks only on one surface of the PNTD layer and the spectrum from particles that produced tracks on both the top and bottom surfaces of the PNTD layer. For a particle to produce tracks on both the top and bottom surfaces of the PNTD, it must possess a range in excess of the pre-etch thickness of the layer—in this case ~600 μm. These particles are most likely High Z and Energy (HZE) particles in primary GCR and the longer range projectile fragment secondaries produced in nuclear interactions between the HZE GCR primaries and the nuclei of the spacecraft and its contents. Particles that form tracks on only a single surface of a PNTD layer have shorter range and are likely either primary protons or short-range target fragment secondaries produced in proton and neutron interactions with nuclei in or near the PNTD layer. The minimum range of a particle that can form a measurable track in CR-39 PNTD is on the order of the bulk etch, the thickness of bulk detector removed during chemical etching. For the long-etch, this is ~40 μm, meaning that target fragment secondaries with range less than 40 μm will not be detected in the long-etch PNTD layer. The bulk etch for the short-etch PNTD layer is ~8 μm and *the differential fluence spectrum from the short-etch detector above 100 keV/μm shows more tracks than do either of the two long-etch spectra. This demonstrates that short-range target fragments make a significant contribution to the LET spectrum at high LET.*

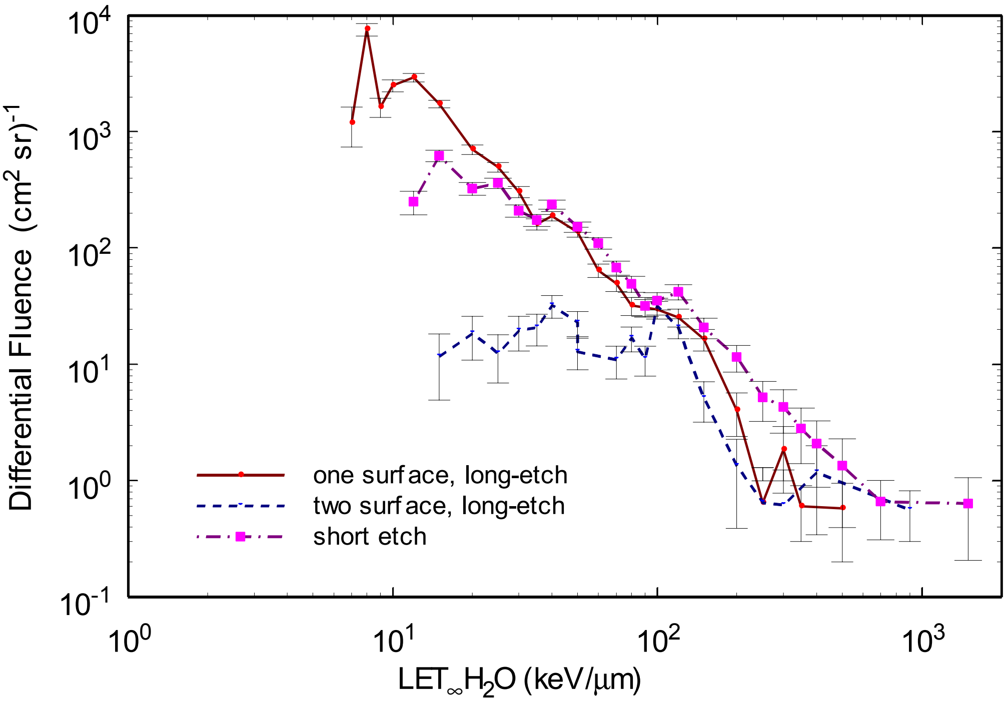

Figure 2. Differential LET fluence spectra from one surface (protons, short-range secondaries) and two surface (HZE particles) measurements in the long-etch CR-39 PNTD from the A0105 PDS dosimeter. Also shown is the differential LET fluence spectrum measured in the short-etch CR-39 PNTD from the A0105 PDS dosimeter.

Figure 3 shows the average integral LET flux spectra measured in the three mutually-orthogonal long-etch CR-39 PNTD layers and the three mutually-orthogonal short-etch CR-39 PNTD layers of PDS Dosimeter A0105. The short-etch spectrum from the z-axis extends to significantly higher LET than does that from the z-axis long-etch spectrum, illustrating the contribution to the LET spectrum at high-LET from short-range target fragment secondaries. Similarly, the short-etch spectra in both the x- and y-axes lie above those measured in the long-etch detectors. The short-etch tracks that populate the high-LET region of the spectrum are believed to be the result of neutron- and proton-induced target fragment interactions with the C and O nuclei of the detector itself. The long-etch spectra extend to lower LET than do the short-etch spectra, due to the difficulty in locating and accurately measuring the small, low-LET tracks in the short-etch detector. There is little difference in the long-etch spectra measured in the three different orientations, indicating that there was little difference in the shielding distributions is these three directions. The lack of difference in the LET spectra measured in the three orientations seen *for the PDS Dosimeter A0105 also held for the other eleven PDS dosimeters. However, differences in the angular distribution of shielding surrounding the PDS dosimeters would tend to have been smeared out by the fact that for nearly 20% of the on-orbit period all the CR-39 PNTD stacks were exposed together in the same location, and by the fact that during much of the DOSMAP experiment, the orientation of the ISS relative to the geomagnetic field was not fixed.*

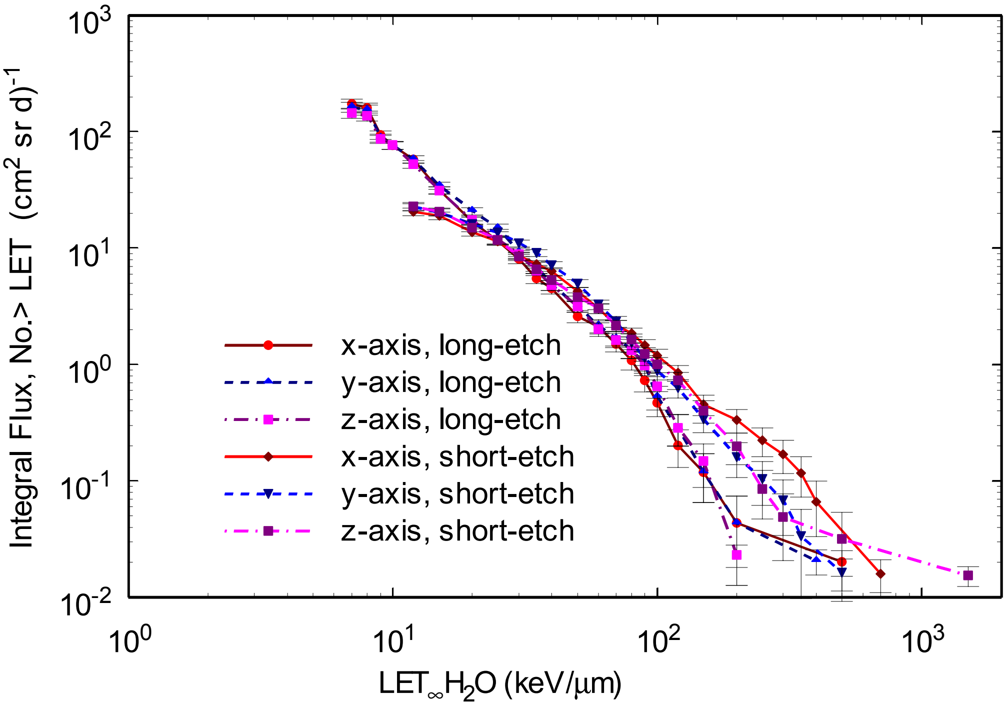

Figure 3. Integral LET flux spectra measured in the three mutually-orthogonal long-etch layers and the three mutually-orthogonal short-etch layers of CR-39 PNTD in the A0105 PDS dosimeter.

Figure 4 shows the average integral LET flux spectra from the combined short-etch and long-etch PNTD layers for PDS Dosimeter A0102, PDS Dosimeter A0104, and PDS Dosimeter A0105. Recall that PDS Dosimeter A0102 possessed the highest average dose rate as measured by TLD, while PDS Dosimeter A0104 possessed the lowest TLD-measured average dose rate. What is remarkable is the lack of difference in the integral LET flux spectra measured in these three locations. In general, there was very little difference seen between the LET spectra measured at all twelve PDS locations. In part, this lack of difference can be explained by the fact that for 20% of the on-orbit time, the CR-39 PNTD stacks in all twelve sets of PDS dosimeters were exposed in the same location. In addition, during the 2001 time period, the ISS had only been partially assembled and was filled with only a minimum of equipment and supplies that would have provided additional shielding. Finally, many of the PDS dosimeter exposure sites, e.g. near the forward and aft hatches of the ISS modules, likely possessed three-dimensional shielding distributions that were quite similar.

Table 1 lists the average dose and dose equivalent rates from particles of LET∞H_2O ≥10 keV/μm measured in the twelve sets of CR-39 PNTD, together with the average total dose and dose equivalent rates from the twelve PDS dosimeters obtained by combining the absorbed dose measured in the Pille TLD cells, with the dose and dose equivalent measured in CR-39 PNTD. Average dose rate from particles of LET∞H_2O ≥10 keV/μm among the twelve PDS dosimeters range from a minimum of 17.5 μGy/d to a maximum of nearly 30 μGy/d, while the average dose equivalent rate from ≥10 keV/μm particles range from 201.6 μSv/d to 232.8 μSv/d. Average total dose rate from combined TLD and CR-39 PNTD measurements ranged from 165.1 to 248.7 μGy/d, while average total dose equivalent rate ranted from 337.2 to 451.4 μSv/d. In general, there was little correlation between the extremes in dose rate and dose equivalent rate from ≥10 keV/μm particles as measured in CR-39 PNTD. There was only a weak correlation between absorbed dose rate as measured by the Pille TLD cells and the average total dose and dose equivalent rates from the combined CR-39 PNTD and Pille TLD measurements. Some of this lack of correlation reflects the fact that the CR-39 PNTD stacks were exposed for a longer duration than were the Pille TLD cells and that during this additional exposure time, the CR-39 PNTD stacks were exposed in the same location. However, this lack of correlation also illustrates the overall complexity of the space radiation environment encountered aboard LEO spacecraft and the fact that the LEO space radiation environment is made of a number of distinct radiation components.

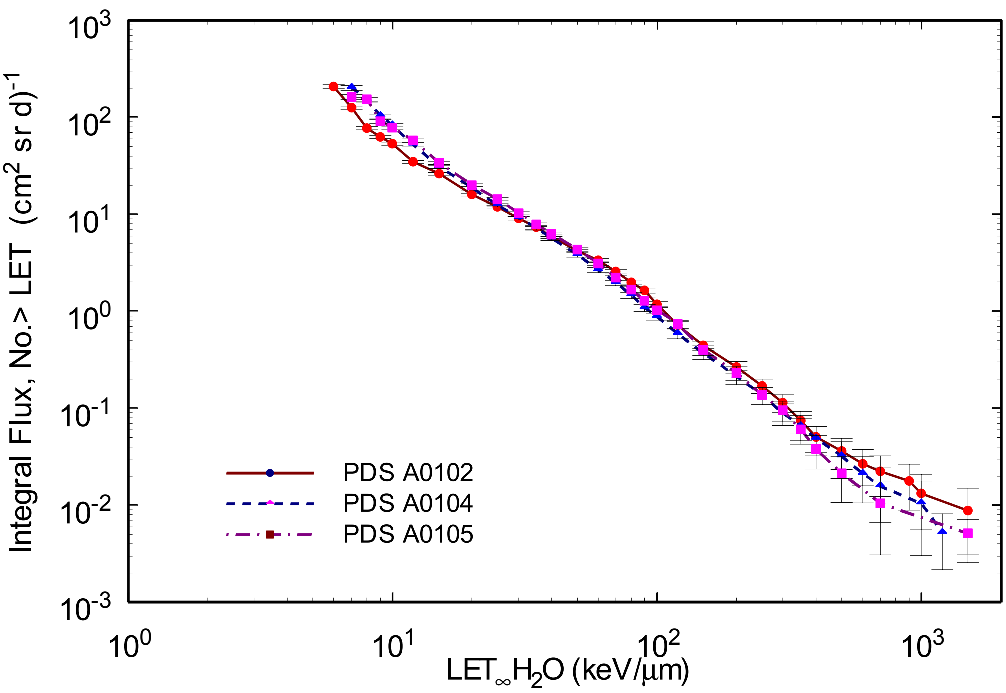

Figure 4. Integral LET flux spectra measured by CR-39 PNTD in the three of the twelve PDS dosimeters during the Expedition 2 DOSMAP Experiment.

Conclusions

The combination of TLD and CR-39 PNTD used in the ISS Passive Dosimetry System provides sensitivity to the major components of the space radiation environment of relevance to space crew dosimetry. Use of the Pille on-board TLD system means that the Pille TLD cells can read out and annealed by the ISS crew on orbit for any time period or condition, meaning that dose information for EVA or following a solar particle event is available when needed. The small size and mass, and the lack of a power requirement permits relatively large numbers of PDS dosimeters to be employed throughout the habitable volume of the ISS at any one time. The performance of the PDS was found to be comparable to other active and passive radiation detectors during ground-based testing conducted under the auspices of the InterComparison of Cosmic rays with Heavy Ion Beams at NIRS (ICCHIBAN) project [Uchihori et al., 2002; Uchihori & Benton, 2004].

Results from the 2001 Expedition 2 DOSMAP experiment, the first on-orbit experiment to use the PDS, illustrate the general effectiveness of the system for area dosimetry on ISS. LET spectrum measurements using a combination of long-etch and short-etch CR-39 PNTD layers demonstrated that short-range, high-LET secondary particles make a significant contribution to dose and dose equivalent in LEO and should not be neglected when making dosimetric measurements on ISS. The differences in average dose and dose equivalent rates from particles of $LET_\infty H_2O \geq 10$ *keV/μm, as well as in average total dose and dose equivalent rates, illustrate the overall complexity of the space radiation environment on the interior of spacecraft and the many variables, including the three dimensional shielding distribution at any one location inside ISS and the orientation of the ISS relative to the trapped protons in the South Atlantic Anomaly, that affect the dose and dose equivalent rate in LEO.*

References

Apathy, I., Deme, S. and Feher, I. (1996) "Microprocessor controlled portable TLD system," Rad. Prot. Dos. 66 301-304.

Benton, E. R. and Benton, E. V. (2001) "Space radiation in low-Earth orbit and beyond," Nuc. Inst. & Meth. B 184 255-294.

Benton, E. R., Benton, E. V. and Frank, A. L. (2002) "Passive dosimetry aboard the Mir Orbital Station: internal measurements," Rad. Meas. 35(5) 443-460.

Deme, S., Apathy, I.., Feher, I., Akatov, Yu., Reitz, G., and Arkhangelski, V. (2006) "Doses due to extravehicular activity in space stations," these proceedings.

Feher, I., Deme, S., Szabo, B., Vagvolgyi, J., Szabo, P. P., Csoke, A., Ranky, M. and Akatov, Y. (1981) "A new thermoluminescent dosimeter system for space research," Adv. Space Res. 1 61-66.

International Commission on Radiological Protection (1991) 1990 Recommendations of the International Commission on Radiological Protection, Pergammon, Oxford, UK, 60.

Noll, A., Rusch, G., Rocher, H., Dreute, J. and Heinrich, W. (1988) "The Siegen automatic measuring system for nuclear track detectors: new developments," Nuc. Tracks & Rad. Meas. 15 (1-4) 265-268.

Rusch, G., Winkel, E., Noll, A. and Heinrich, W. (1991) "The Siegen automatic measuring system from track detectors: new developments," Nuc. Tracks & Rad. Meas. 19 (1-4) 261-266.

Uchihori, Y., Fujitaka, K., Yasuda, N., Benton, E. R., and the ICCHIBAN Collaboration (2002) "Intercomparison of Radiation Instruments for Cosmic-rays with Heavy Ion Beams at NIRS (ICCHIBAN Project)", J. of Rad. Res. 43, S81-S85.

Uchihori, Y. and Benton, E. R. (2004) Results from the first two InterComparison of dosimetric instruments for Cosmic radiation with Heavy Ion Beams at NIRS (ICCHIBAN-1 & -2) Experiments, National Institute of Radiological Sciences, Chiba, HIMAC-078.

Table 1. Average dose and dose equivalent rates measured by TLD, CR-39 PNTD, and the combination of the two detectors in the twelve PDS dosimeters exposed aboard ISS during the Expedition 2 DOSMAP experiment. Also listed are the locations of the twelve PDS dosimeters within the Node 1 and U.S. Lab modules.

PDS Dosimeter No.	Exposure Location	Pille TLD Dose Rate (μGy/d)	≥10 keV/μm Dose Rate (μGy/d)	Total Dose Rate (μGy/d)	≥10 keV/μm Dose Equivalent Rate (μSv/d)	Total Dose Equivalent Rate (μSv/d)
A0101	US Lab, HRF Rack in Pille Reader	239.5 ± 1.7	24.7 ± 1.0	245.0 ± 12.7	226.8 ± 10.1	447.1 ± 25.9
A0102	Node 1, Zenith near aft hatch	242.6 ± 19.0	22.1 ± 0.7	248.7 ± 13.0	225.1 ± 10.3	451.4 ± 26.6
A0103	US Lab, HRF Rack near DOSTEL	180.5 ± 11.8	29.8 ± 1.2	184.8 ± 11.0	232.8 ± 12.0	389.3 ± 24.0
A0104	Node 1, Zenith area of forward hatch	160.8 ± 9.1	29.3 ± 1.2	165.1 ± 10.1	201.6 ± 9.8	337.4 ± 22.3
A0105	Node 1, Zenith area of starboard hatch	191.5 ± 13.2	29.8 ± 1.2	196.1 ± 11.3	230.6 ± 10.6	397.2 ± 24.7
A0106	Node 1, Port side close to US Lab	169.9 ± 13.2	20.9 ± 1.0	174.2 ± 10.3	189.6 ± 10.1	343.0 ± 23.5
A0107	US Lab, Zenith area of aft hatch	169.4 ± 11.5	17.5 ± 0.7	173.0 ± 11.3	181.7 ± 9.8	337.2 ± 24.2
A0108	Node 1, Nadir area on forward hatch	175.4 ± 13.7	21.6 ± 0.7	178.1 ± 9.6	218.6 ± 10.3	377.5 ± 22.8
A0109	US Lab, starboard side near forward hatch	178.8 ± 16.3	24.2 ± 1.0	183.1 ± 10.8	204.0 ± 10.1	362.9 ± 23.8
A0110	US Lab, starboard side close to aft hatch	173.5 ± 13.7	21.4 ± 1.0	178.6 ± 10.6	219.6 ± 10.8	376.8 ± 24.2
A0111	US Lab, port side close to forward hatch	183.6 ± 18.7	19.0 ± 0.7	187.4 ± 10.1	189.1 ± 9.4	357.6 ± 22.6

A0112	*US Lab, port side near aft hatch*	*161.0 ± 9.1*	*19.2 ± 0.7*	*165.4 ± 9.4*	*200.4 ± 9.8*	*346.6 ± 221*